791017

Child Restraint Evaluation by Experimental and Mathematical Simulation

J. Wismans and
J. Maltha
Research Institute for Road Vehicles
TNO-Delft (Holland)

J. W. Melvin and
R. L. Stalnaker
Biomechanics Department Highway
Safety Research Institute
University of Michigan

Abstract

Two child restraint system sled tests with a child cadaver* and a 3-year old child dummy have been carried out at the Highway Safety Research Institute of The University of Michigan. Some differences between the kinematical response of dummy and cadaver were found. Two mathematical models have been formulated, using the MADYMO program package, for the special purpose of evaluating child restraint performance. A description of the validated dummy and cadaver model is presented

*The protocol for the use of the cadaver in this study was reviewed by the Committee to Review Grants for Clinical Research and Investigation Involving Human Beings of The University of Michigan Medical Center and follows guidelines established by the U.S. Public Health Service and recommended by the National Academy of Sciences/ National Research Council.

0585-086X/79/1017-1017/$02.50

together with a comparison of experimental and model results. A sensitivity study was conducted to have a better insight into the effects of various parameters on the child's response. To show the use of the model as a design tool, a simulation with an energy absorbing backstrap is presented. It is concluded that the mathematical model is a better simulation for the cadaver kinematics than the dummy.

THE LABORATORY EVALUATION of child restraint system performance has almost exclusively relied upon the use of child-size test dummies, subjected to impact sled or car crash tests. Child restraint system designs exhibit widely varying configurations with restraint concepts ranging from simple belt harnesses to padded impact shields. Improvement and optimization of child restraint crash protection is impeded by a lack of biomechanical information on the kinematics and impact tolerance of children and by lack of a simple economical method for studying restraint system performance. Mathematical models of child occupants in restraint systems could prove to be very effective in overcoming some of these impediments by providing a means of systematically studying various features of child restraint designs prior to actually building and testing of real systems. Also, mathematical models can be used to interpret and enhance biomechanical data that can be obtained from limited experiments and accident reconstructions and as an aid to improving child dummy design.

Mathematical simulation of the gross motion of the human body in a dynamic impact environment has become a very active research objective in the last fifteen years. The development of these crash victim models has been primarily concentrated on the adult male. The only available data for dynamic impact child models were reported in freefall studies (1)*, where the model construction was based on scaling and interpolating procedures of the existing adult occupant MVMA-2D model.

Similarly, cadaver testing in an impact environment has been going on for many years. The biomechanical data obtained from these tests has contributed greatly to the understanding of impact tolerance of the adult human. To date, the only biomechanical data available on restrained child cadavers in well-instrumented and well-defined crash conditions were reported by Kallieris (2).

The experimental work to be reported here, was carried out in 1977 at the Highway Safety Research Institute of the University of Michigan and consists of two sled tests,

*Numbers in parentheses designate References at end of paper.

one with a 3-year old child dummy (Alderson Research Laboratory, Part 572)** and one with a 6-year old child cadaver (with approximately the anthropometry of a 4-year old child), both restrained in separate Strolee Wee Care child restraint systems.

The modeling work reported here consists of the development and validation of two 2-dimensional mathematical models (dummy, cadaver) of a restrained child in a frontal impact, as an attempt to combine and extend these two areas of study.

In future this methodology will be extended to reconstructions of real accidents (3). So cadaver, dummy and model simulation can work together to give a better understanding of a particular accident situation and to supply valuable tolerance information.

EXPERIMENTAL METHODS

CADAVER TEST - The cadaver test subject used in the experiment was a 6-year old male child that had died of acute bronchopneumonia. The physical development of the subject had been retarded due to a hydrocephalic condition and was approximately that of a four year old child. The height and weight of the cadaver was 11-12% greater than that of the 3-year old child test dummy and the seated height was approximately 5% greater than the dummy. The cadaver was prepared for testing using procedures developed at HSRI for whole-body impact testing of adult cadavers (4). These procedures include the following features:

1. Comprehensive anthropometry of the subject.
2. Pre-test radiographic documentation of skeletal condition.
3. Attachment of head and spinal accelerometer mounts.
4. Installation of vascular and airway pressurization tubes.

The head acceleration measurement used the 9-accelerometer method with three individually mounted triaxial clusters (5). Each cluster uses three uniaxial piezoresistive miniature accelerometers (Endevco 2264-2000) situated in three orthogonal directions. The mounts were located laterally on the left and right parietal bones and centrally on the frontal bone. The acceleration of the spine was measured using a triaxial accelerometer cluster mounted on the eighth thoracic vertebra. The mount was attached such that the accelerometers were oriented in the three anatomical directions (anterior-posterior (A-P),

**Proposed specifications and performance requirements for anthropomorphic test dummy representing three year old children (49 CFR part 572, May 18, 1978).

left-right (L-R) and superior-inferior (S-I).

The airway pressurization tube was inserted into the trachea through an incision at the base of the front of the neck and the vascular system pressurization catheter was inserted through an incision in the common carotid artery. The basic pressurization techniques have been described previously (6). The thoric pressure was measured during the impact, but not the lung pressure.

Following surgical preparation, the cadaver was dressed in cotton thermal underwear similar to that used in standard child seat testing with dummies. The cadaver was transported to the sled facility and seated in a Strolee Wee Care child restraint (see Fig.1) which was installed on a bench seat for child restraint testing (7). The child restraint was attached to the vehicle seat by a car lap belt and with its special top tether strap. Seat belt load cells (GSE Type 2500) were used on the right and left car lap segments, the top tether strap and the right and left shoulder straps of the child restraint five-point harness system.

The sled impact test was conducted according to the test procedures specified in the proposed FMVSS 213 (March 1974). A sled deceleration-time profile of nominally 30 mph (50 kph) velocity change with an average deceleration of 20 G was used. In addition to the electronic data recorded from the transducers in this test, high-speed movies (1000 frames/sec) were taken to document the kinematics of the test subject. After the test, the subject was returned to the surgical area and an autopsy was conducted to examine the cadaver for possible injury.

DUMMY TEST - Following the test with the cadaver, a second child restraint was installed on the bench seat and the test was repeated using the Part 572 3-year old child dummy. The dummy was instrumented with an internal triaxial cluster of accelerometers in the head and chest. The belt load cell arrangement was the same as used in the cadaver test. All other aspects of the sled test were identical to those used in the cadaver test.

MATHEMATICAL SIMULATION

GENERAL - In a mathematical impact simulation of a child in a restraint system, the dynamic behavior of the child, as well as that of the restraint system has to be considered. The child interacts with the restraint system, while the restraint system interacts with the vehicle seat. In the presented models, child and restraint system are simulated by two separate systems: the dummy (cadaver) model, represented by a linkage of seven (nine) masses; and the restraint system, represented by a single-mass system.

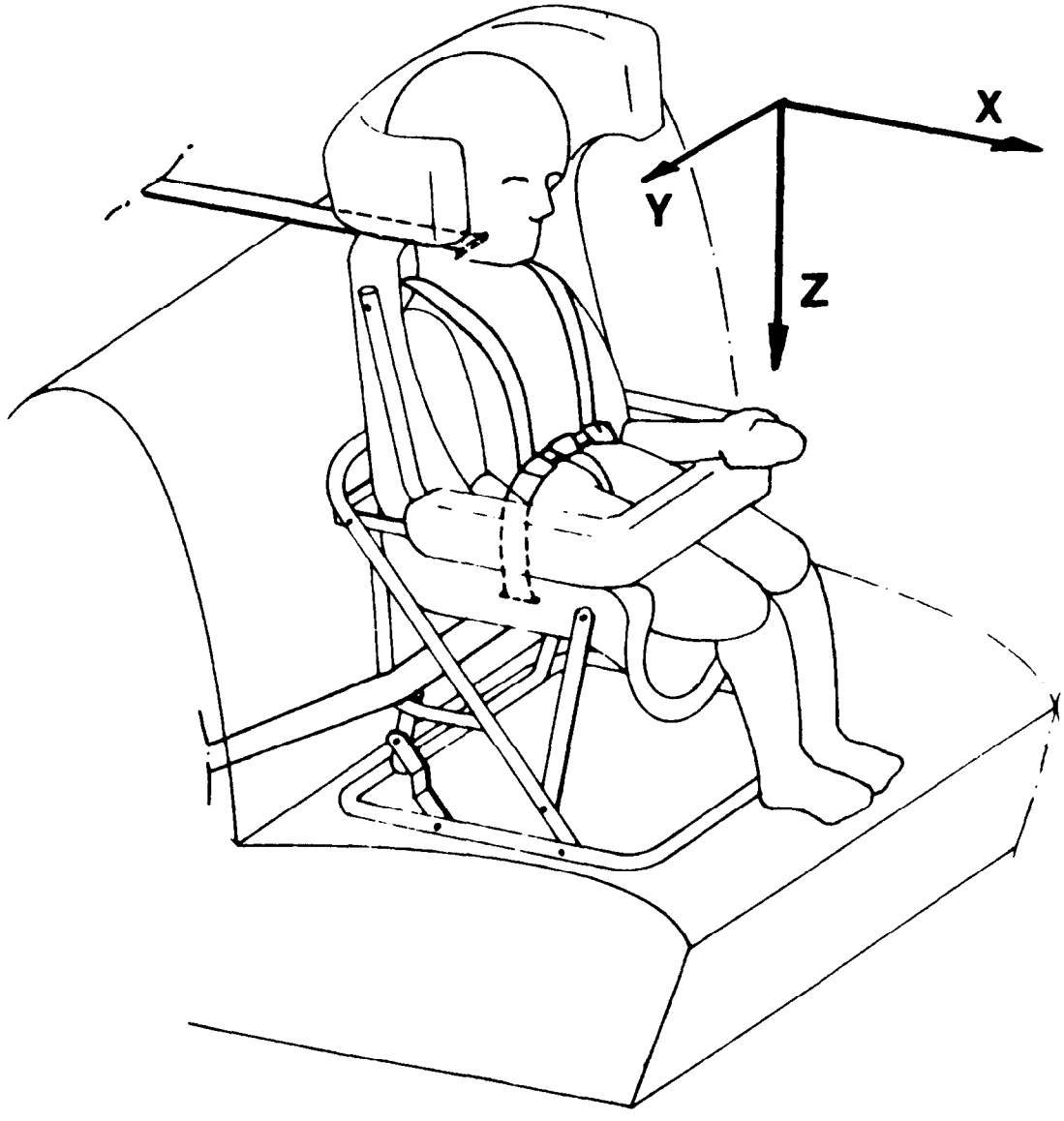

Fig. 1 - Overall view of test set-up and orientation of a XYZ co-ordinate system

The force interactions between the restraint system and the child; and the restraint system and the vehicle are simulated by a number of springs, representing belts and ellipse-plane models, representing geometrical contacts. These simulations are restricted to motions in the X-Z plane (Fig. 1).

A review of several computer programs now available for simulation of human body gross motion is given by Robbins (8). Except for the CALSPAN 3D CVS program (9), these models have a specified number of connected rigid masses, all belonging to one linkage system. The MADYMO CVS program package (10) is used for the work presented here. This new program, which was not considered in the study of Robbins, contains a two- and a three-dimensional option, with the following characteristics:

(1) An arbitrary number of linkage systems with a variable number of elements.

(2) Automatic generation of the equations of motion;

(3) Standard force interaction routines for resistive joint torques, deceleration field, and belt and contact forces.

(4) A possibility for the users to define their own force interaction routines.

A general description of the model formulation is given in the following sections, with a more detailed description in reference (11).

FORMULATION OF THE MODEL

Dummy model - A side view of the 3-year old child dummy is shown in Figure 2. The relevant dimensions for the formulation of the two-dimensional dummy model were measured with an accuracy of 0.01 m. The measurement of the weights, centers of gravity and moments of inertia were done with all of the bolts threaded into their mating parts, rather than remaining with the pieces they held in place.

The center of gravity of the long elements, like the arms, legs, etc. was measured by balancing these segments on a knife-edge. The center of gravity for the other elements, like head, thorax, etc. was determined by free hanging of the element in two positions by a cord. The accuracy of these methods is 0.01 m.

The moment of inertia of the dummy parts about an axis through the center of gravity and perpendicular to the X-Z plane was measured with a torsional pendulum (12,13) (Table 2). A check of the accuracy of this method was done by measuring several well-defined objects. Depending on the magnitude of the moments of inertia, the accuracy varies between 1 and 2 %. The moment of inertia of the torso foam and skin could not be measured by this method, so this value had to be estimated.

The dummy model consists of 7 elements: head, torso 1,

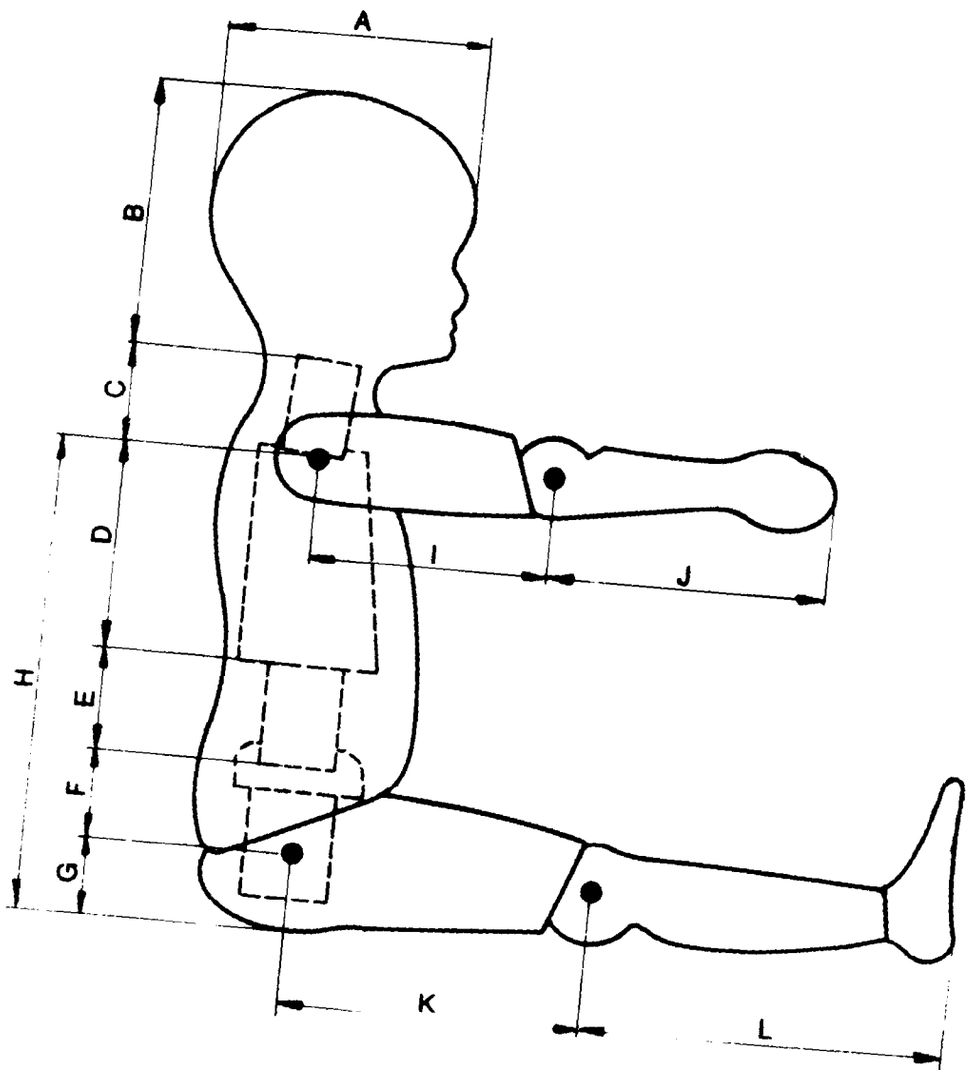

Fig. 2 - Side view of child occupant with dimensions (refer to Table 1)

Table 1 - Some Dimensions of the Dummy and the Cadaver (refer to fig.2)

	Dummy m	Cadaver m
Stature	0.98	1.091
Sitting height	0.571	0.6
A	0.175	0.134
B	0.170	0.19
C	0.081	0.05
D	0.115	-
E	0.08	-
F	0.065	-
G	0.06	0.04
H	0.32	0.36
I	0.125	0.16
J	0.24	0.25
K	0.23	0.26
L	0.245	0.28

Table 2 - Mass and Moment of Inertia of the Dummy Segments of a Three Year Old Child Dummy (type Alderson).

Segment	Mass kg	Moment of Inertia kgm^2
Head	2.64	13.0×10^{-3}
Neck upper torso component	0.46	0.76×10^{-3}
Upper torso component	0.70	10.6×10^{-3}
Torso skin and foam	2.67	4.0×10^{-3}
Spine	0.79	0.96×10^{-3}
Upper and lower pelvis	1.51	3.7×10^{-3}
Upper arms + hands	0.64	2.7×10^{-3}
Lower arms	0.51	3.7×10^{-3}
Upper legs	3.54	23.1×10^{-3}
Lower legs + feet	1.39	9.8×10^{-3}

torso 2, upper arm, lower arm, upper leg and lower leg. These elements were connected by 6 hinge joints: the neck, shoulder, elbow, spine, hip and knee joint (Fig. 3).

The shoulder, hip, elbow and knee joint were located, corresponding to the positions of these joints in the dummy, while the neck joint and the spine joint were located at the center of gravity of the undeformed rubber cilinders, representing neck and spine.

The mass of the dummy segments was assigned to the model elements as given in Table 3. The resulting mass, length, moment of inertia and location of center of gravity of the model elements are presented in Table 4 and Table 5. It was found that the positions of the center of gravity were within 0.01 m of a line connecting the joint centers, so these ofset distances were assumed to be zero.

The static resistance (stiffness) to rotation (including range of motions and joint stops) of the dummy joints was determined. The frictional resistance to motion in the shoulder, elbow, hip and knee were set to zero for measuring these data. The resulting characteristics were approximated by linear functions as shown in Figure 4.

In the experiment the friction in the shoulder, elbow, hip and knee joints were adjusted to a one-g level. In the model these frictional torques were described by a constant level of torques that opposes relative joint motion (Table 6).

Finally, a velocity dependent resistive torque (viscous damping) was defined for all of the model joints. The values for the viscous damping coefficients were based on observations that the shoulder, elbow, and knee were almost critically damped, while the damping in the neck, spine and hip joints was estimated to be lower than critical. The values used in the model are given in Table 6.

Cadaver Model - The relevant dimensions of the child cadaver, which were selected from standard anthropometric measurements (accuracy of 0.01 m) are presented in Table 1.

Analysis of the cadaver experiment show a complicated head-neck-torso motion and rather large deformations of the spine in comparison to the dummy experiment (Fig. 5). It was felt that the 7-mass dummy model was not sufficient to describe these kinematics, so for the cadaver model two extra elements were introduced: a neck element and a third torso element (Fig. 3). The upper neck and lower neck pivots were located at the occipital condyles and C_7-T_1 articulations, respectively. The torso was devided into three equal elements.

The length of the cadaver model elements was selected from the anthropometric measurements. The element masses, locations of the center of gravity and moments of inertia were determined by extrapolation and estimations from mass

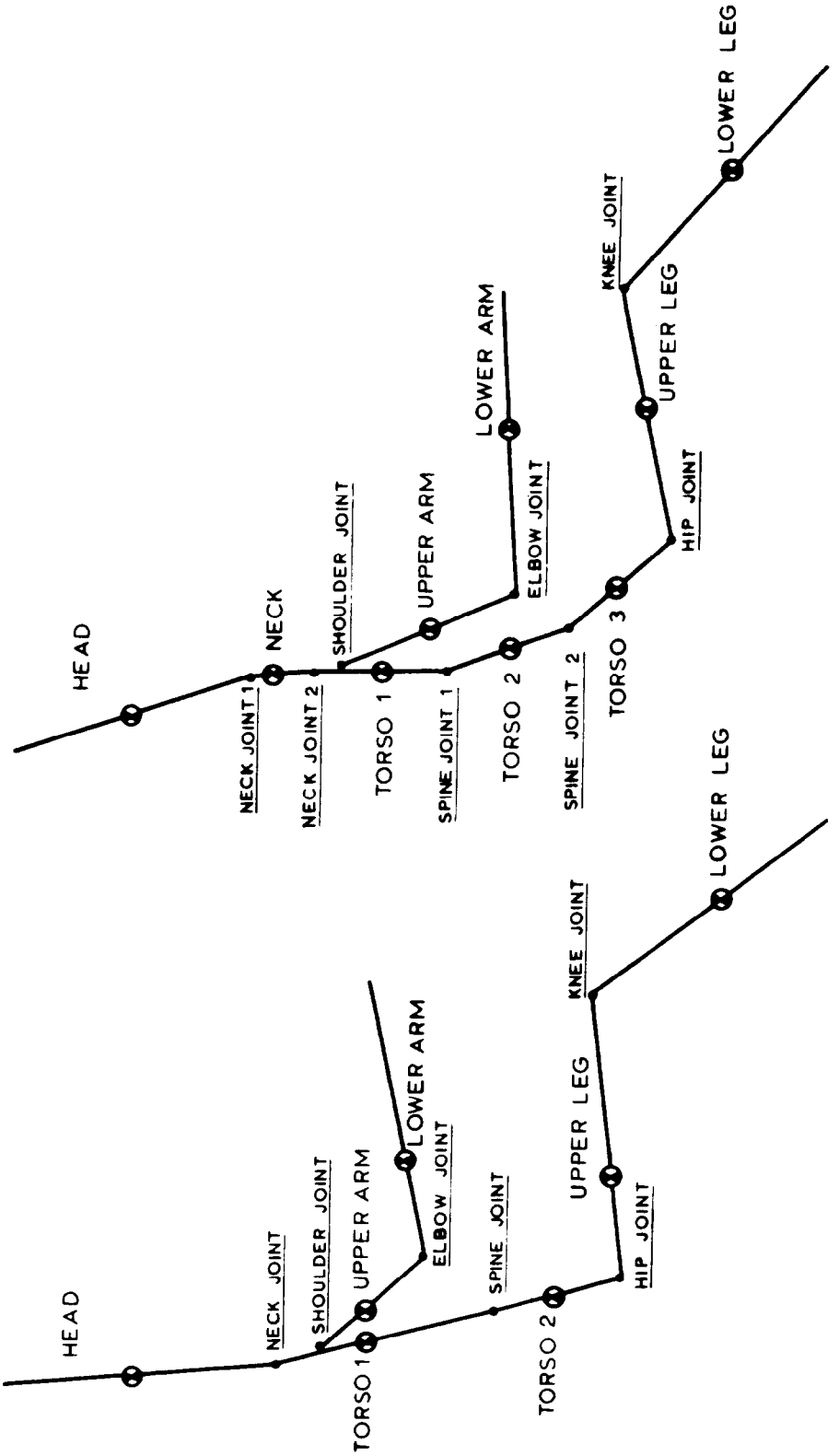

Fig. 3 - A 7-mass dummy model and a 9-mass cadaver model

Table 3 - Assignment of Dummy Segment Masses to Dummy Model Elements.

Model Element	Dummy Segment
Head	head + $\frac{1}{2}$ neck
Torso 1	upper torso component + $\frac{1}{2}$ neck + $\frac{1}{2}$ spine + $\frac{1}{2}$ torso foam and skin
Torso 2	upper and lower pelvis + $\frac{1}{2}$ spine + $\frac{1}{2}$ torso foam and skin
Upper arm	two upper arms
Lower arm	two lower arms and hands
Upper leg	two upper legs
Lower leg	two lower legs and feet

Table 4 - Length of the Model Elements and Location of the Centers of Gravity.*

	Dummy		Cadaver	
Element	Length m	c.g. m	Length m	c.g. m
Head		0.125		0.085
Neck			0.05	0.015
Torso 1	0.190	0.080	0.11	0.050
Torso 2	0.105	0.055	0.11	0.055
Torso 3			0.11	0.045
Upper arm	0.125	0.055	0.16	0.080
Lower arm	0.240	0.085	0.25	0.110
Upper leg	0.230	0.080	0.26	0.13
Lower leg	0.245	0.135		0.14

*Distance to neck joint for the head and distance to proximal joint for the other elements.

Table 5 - Mass and Moment of Inertia (I_y) of the Model Elements.

Element	Dummy Mass kg	Dummy I_y kgm^2	Cadaver Mass kg	Cadaver I_y kgm^2
Head	2.87	13.3×10^{-3}	2.64	8×10^{-3}
Neck			0.32	0.2×10^{-3}
Torso I	3.64	16.1×10^{-3}	2.77	7×10^{-3}
Torso II	2.26	5.5×10^{-3}	2.00	5×10^{-3}
Torso III			2.48	7×10^{-3}
Upper arm	0.64	2.7×10^{-3}	0.70	1.2×10^{-3}
Lower arm	0.51	3.6×10^{-3}	0.76	1.2×10^{-3}
Upper leg	3.54	23.1×10^{-3}	3.22	17×10^{-3}
Lower leg	1.39	9.8×10^{-3}	1.72	8×10^{-3}
Total	14.86		16.61	

Table 6 - Joint Friction and Damping Characteristics for the Dummy resp. Cadaver Model.

Joint	Dummy C_1 Nm	Dummy C_2 Nm sec/rad	Cadaver C_1 Nm	Cadaver C_2 Nm sec/rad
Neck 1	0	1	0	0.5
Neck 2			0	0.5
Spine 1	0	2	0	0.5
Spine 2			0	0.5
Shoulder	1.36	0.35	0	0.1
Elbow	0.41	0.1	0	0.1
Hip	5.90	1	0	0.1
Knee	1.83	0.5	0	0.1

C_1 = Coulomb friction torque
C_2 = Viscous damping coefficient

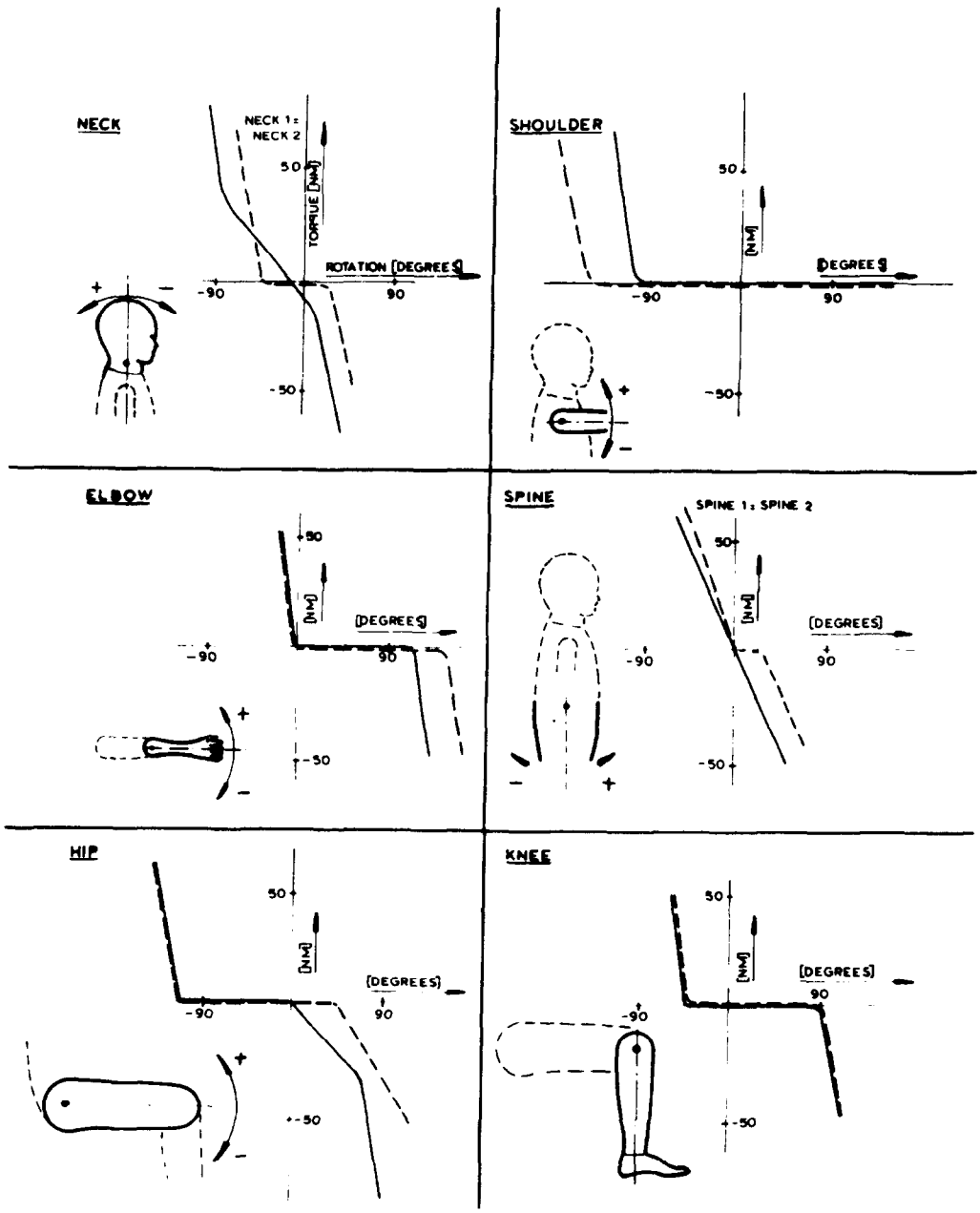

Fig. 4 - Stiffness and "joint stop" characteristics of the joints ——— dummy model ----- cadaver model

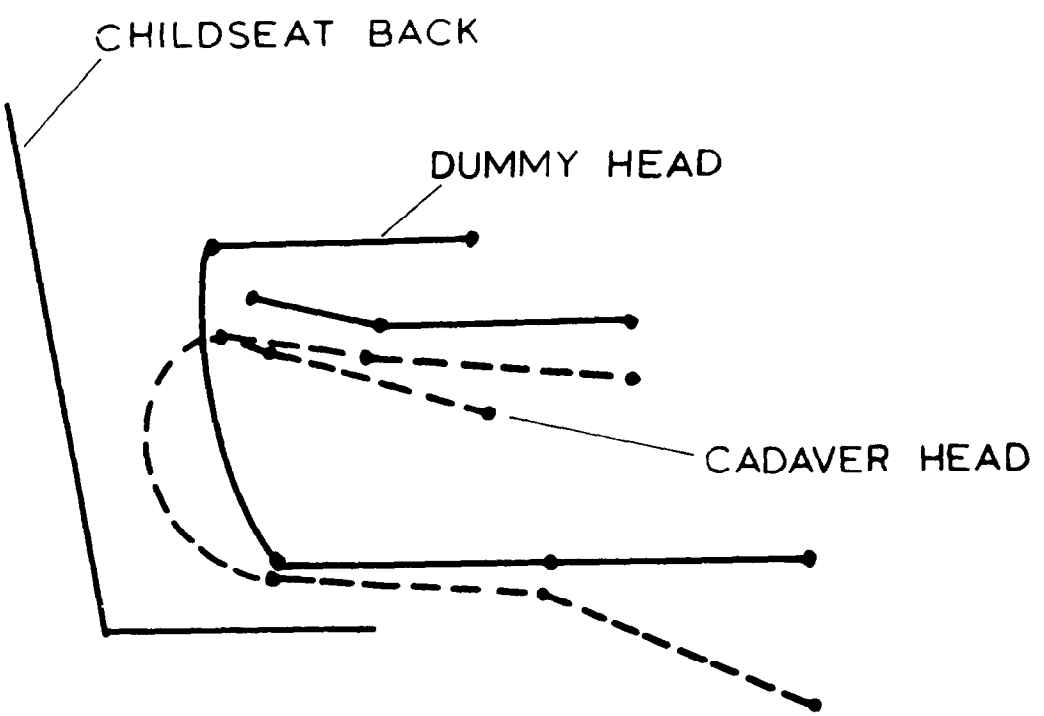

Fig. 5 - Positions of dummy and cadaver relative to the child seat at 80 ms

distribution data of Reynolds (14). The resulting values are given in Tables 4 and 5.

No realistic data are available for the joint characteristics of child cadavers at this time. Based on observations on adult cadavers (4), friction in the cadaver model joints was assumed to be zero, while damping coefficients were set to a lower value than for the dummy model joints (Table 6). Approximately identical stiffness and joint stop characteristics for the shoulder, elbow, hip and knee were introduced for the cadaver model as for the dummy model, with some corrections for the expected increase in the range of motion of the cadaver (Fig. 4). Free motion was introduced for the joints representing the neck and spine of the cadaver, until an elastic stop was encountered.

Model of Child Seat - The child seat was represented in the model by a rigid single-mass system. The mass of the child seat was 5.85 kg and the moment of inertia was 0.24 kgm^2 about an axis through the center of gravity. The center of gravity was 0.26 m above the base of the restraint system and 0.13 m forward of the most rearward point of the base of the seat.

Model of Belts and Harness - The dummy (cadaver) was restrained by a 5-point harness system, connected to a child seat while the child seat was restrained to the vehicle by a standard 2-point adult lap belt and a back strap. With the existing belt force interaction routine in MADYMO, a belt system can be simulated by an arbitrary number of non-linear springs, with options for permanent deformation, energy dissipation and slipping. These springs had to be connected to elements or to the vehicle.

The locations of the springs used in both the dummy and the cadaver model are shown in Figure 6. The lap belt of the child seat harness, the back strap and the car lap belt were each simulated by a single spring, while the shoulder part of the harness was simulated by two springs:

(1) Spring I connected to the child restraint system and the upper torso element.

(2) Spring II connected to the upper torso element and the lower torso element.

The force-deflection characteristics of harness and vehicle belts were approximated by linear functions obtained from results of dynamic tests (A in Table 7).

These characteristics were corrected to account for out of plane webbing lengths and structural deformations like (C in Table 7):

(1) Deformation of the child seat and the top of the car seat back.

(2) Shoulder and abdominal deflections.

Slipping in the shoulder harness was simulated by the introduction of a friction force in the upper torso element

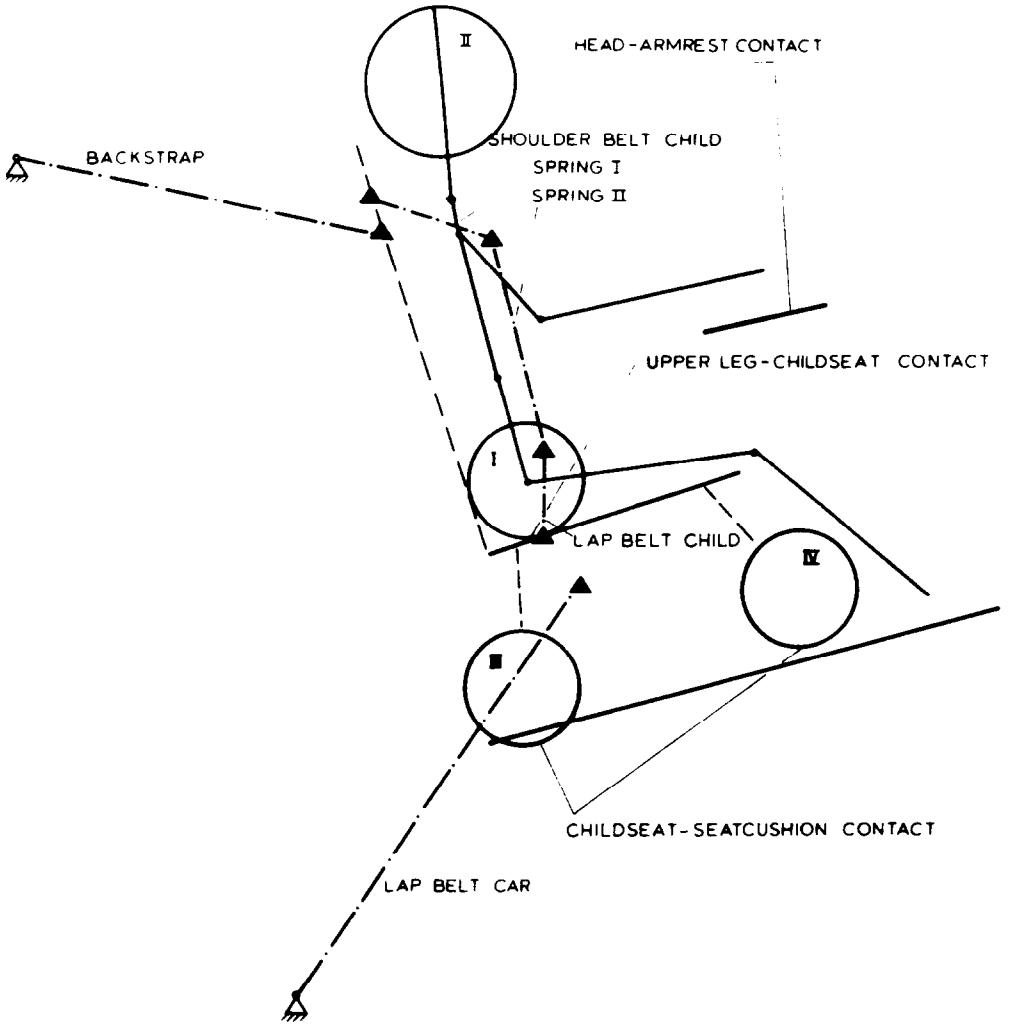

Fig. 6 - Dummy-child seat model with belts and geometrical contacts

anchorage (D in Table 7).

The car lap belt buckle was observed from the film analysis of the cadaver experiment, to slip over the child seat anchorage point during the test. This behavior was simulated in the cadaver model by adjusting the car lap belt characteristics.

Model of Contact Forces - Contact surfaces were defined for the upper leg interacting with the restraint system's seat base, the restraint system interacting with the vehicle seat cushion, and the head interacting with the arm rest. These geometrical contacts were described by four ellipse plane interactions as shown in Figure 6. Static force deflection characteristics of the contact situations were approximated by linear functions (Table 8). Also a velocity dependent resistive force was introduced. The viscous damping coefficients were estimated. Coulomb friction to resist the sliding of upper leg, relative to restraint system's seat; and the seat frame relative, to the vehicle seat cushion was also estimated. The same geometrical contact description was used for the cadaver simulation.

Initial Position - The initial positions, just prior to impact, of the dummy and cadaver were obtained from high-speed movie analysis.

Sled Pulse - The HSRI deceleration pulse was approximated by three straight line segments as indicated in Fig. 7.

VALIDATION METHOD - Validation of a crash victim simulation is established when a decision is made that the model predictions correlate acceptably with observed facts (15). This means that a subset out of the model predictions must be selected; and that a method must be determined by which the decision can be made whether or not the correlation with the simulated experiment is acceptable. This problem of validation, however, is not yet completely solved, so the only way to approach this problem is to follow common practise and good engineering judgement. The kinematics, belt forces, resultant head and chest acceleration of the models and experiments are compared for this study. In the near future more precise defined methods of validation are expected to be available by the work of the Analytical Human Simulation Task Force of the SAE Human Biomechanics and Simulation Subcommittee (HBSS).

SENSITIVITY ANALYSIS - The sensitivity study was undertaken to evaluate the model's response due to the not-well defined model parameters, like the correction factors for structural deformations. An additional run was made with an energy absorbing (EA) backstrap, as an example of one of the uses of the model of a design tool. A backstrap limit load was set at 3400N for 20cm, all other parameters of the model were left unchanged. The analysis are carried out with the dummy model as a reference. Corresponding to the

Table 7 - Parameters to Describe the Belt Behavior.

Belt	A N/%	B %	C —	D —
Backstrap	300	60	x0.75	
Lap belt	600*	60		
Shoulder harness dummy	300	60	x0.33	0.45
Shoulder harness cadaver	300	60	x0.33	0.30
Lap harness	300	60	x0.33	

A = Approximated static stiffness in loading phase as measured with a hydraulic tester.
B = Energy dissipation in the unloading phase.
C = Estimated correction to account for structural deformations.
D = Estimated friction coefficient in upper torso element anchorage.
*The lap belt characteristic in the cadaver model is corrected for buckle slippage.

Table 8 - Force Deflection Characteristics and Friction Coefficients for the Geometrical Contacts.

Contact	Stiffness N/m	Friction Coefficient	Viscous Damping Coefficient Nsec/m
Upper leg-child seat (I)	10000	0.2	100
Head-Armrest (II)	15000		100
Child seat-seat cushion (III,IV)	5000	1	100

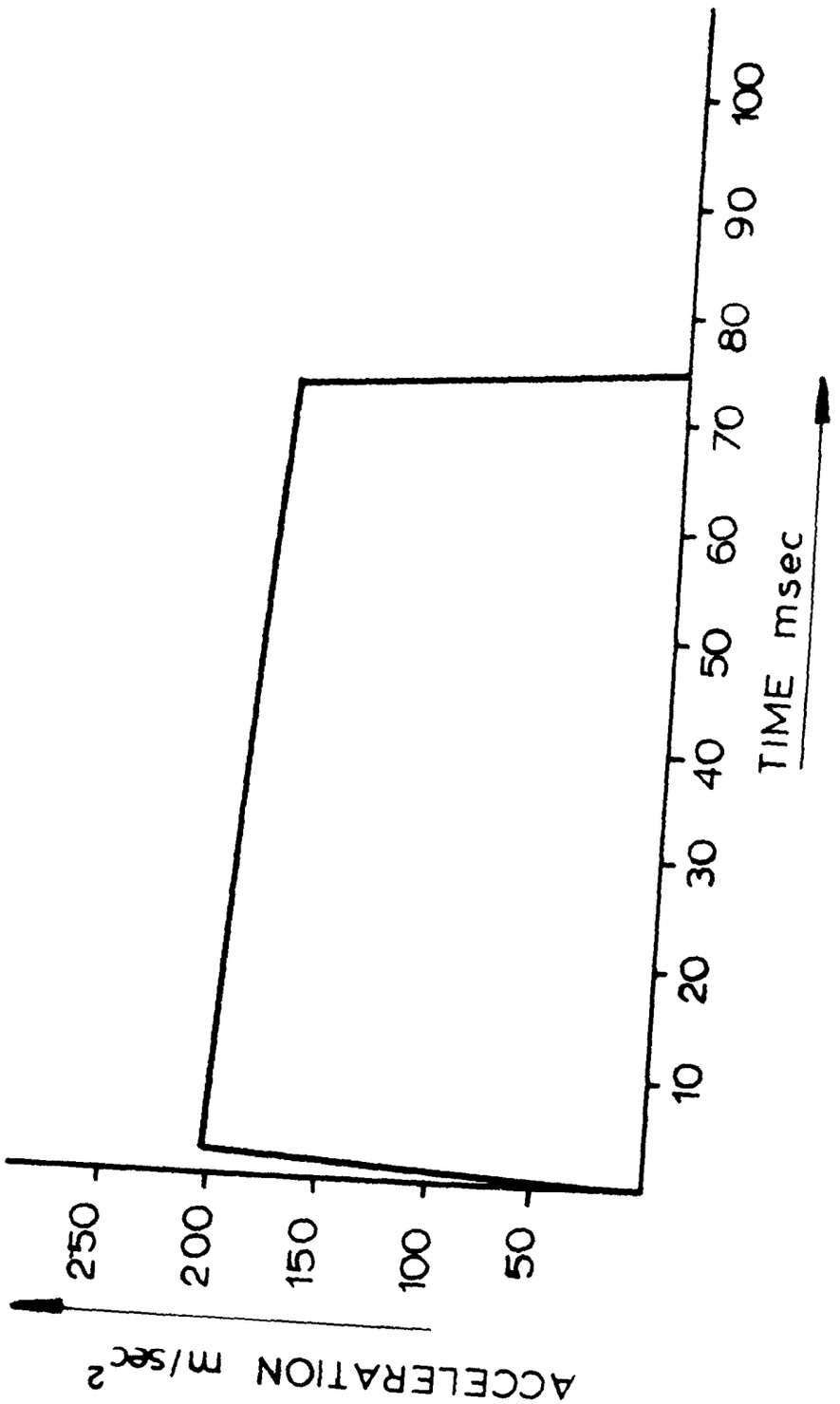

Fig. 7 - Sled deceleration pulseused in the models

studies of Backaitis (16), Peak resultant linear head accelerations were selected as measures of the system's sensitivity; along with peak chest acclerations (for time intervals whose duration is 3 msec or more), maximum head excursions and peak belt loads.

TEST RESULTS

In the interest of keeping this paper compact in format, the test results are presented graphically in conjunction with the section on the model results. This section contains some of the general results, including the results of the autopsy on the cadaver. Because only one test on one cadaver was conducted, only general comments can be made. In general, the peak transducer responses were similar but there were some differences in waveform. Some notable exceptions were in the head accelerations where the peak A-P acceleration of the cadaver was lower (22 G versus 40 G for the dummy) while the S-I acceleration of the cadaver was slightly higher (40 G versus 35 G for the dummy). In the chest the A-P acceleration of the dummy was essentially trapezoidal in waveform with a 30 G plateau while the cadaver A-P acceleration exhibited an early peak of 40 G followed by a lower plateau at 20 G. The vascular pressure time history initially rose like the chest A-P acceleration but then reached a plateau and fell while the acceleration peaked. The pressure peaked at 320 mm Hg after the chest A-P acceleration had fallen to its plateau. The pressure waveform followed the restraint system shoulder harness load history much more closely. The car lap belt waveforms were observed to be different. This was primarily due to slippage of the car lap belt buckle over the child seat anchorage point in the cadaver test.

A detailed autopsy was conducted on the head, neck, chest and abdomen of the cadaver. Prior to dissection, the right side of the thorax was noted to be slightly lower than the left side and more flexible, suggesting rib cage injury. There were abrasions on the shoulders due to the restraint harness. Upon dissection of the thorax an anomalous abbreviated fourth right rib was found which extended only about 5 cm from the sternum. The sternum was intact and there were no rib fractures evident although there was increased bilateral mobility of the anterior ribs. The physicians present at the autopsy thought that the upper chest wall mobility was pronounced enough to have resulted in a possible flail chest condition in the living state. A slight contusion was insignificant. A contusion on the anterior side of the right libe of the liver was noted. There were no other internal injuries. The pelvic region was dissected and examined and no damage was found.

The vertebral column was dissected and the cervical spine was found to have the capsules about the C1/C2 lateral articulations and the atlantoaxial membrane to be very loose but intact. No spinal fractures or dislocations were noted.

There was no evidence that the contact of the face of the cadaver with the restraint system padded bar had caused significant injury. Examination of the brain indicated that its condition during the test precluded any possible injury evaluation due to prior autolysis.

MODEL RESULTS

VALIDATION - The following data of the dummy and cadaver responses were selected for model validation:

(1) High-speed movies.

(2) Force-time functions of the back-strap, the left and right car lap belt and the right and left shoulder straps.

(3) Resultant linear head- and chest accelerations as a function of time.

The resulting kinematics of the experiments and models are plotted in Fig. 8 (dummy) and Fig. 9 (cadaver). The kinematics of the experiments were determined from the high-speed movies with a motion analyser. Because of the absence of markers on the torso, the bending of the spine could not be accurately measured, so in the stick figures of the experiments the torso was represented by a straight line, connecting neck and hip pivots. The child seat and the vehicle seat are each indicated by two line segments. The position of the child seat had to be approximated, because deformations in the child seat of up to 5 cm, were observed. Maximum head excursion and corresponding time to the maximum head excursion are presented in Table 9.

The belt forces and resultant linear head- and chest accelerations for the experiments and the model simulations are shown in Fig. 10 (dummy) and Fig. 11 (cadaver). Maximum linear head- and chest accelerations, their corresponding times, and the HIC are presented in Table 9. The model runs are carried out with time steps of 0.25 milliseconds.

SENSITIVITY STUDY - A complete and detailed documentation of results of the sensitivity study is given in reference (11). In this paper a tabular summary of some results will be presented (Table 10). The analysis was carried out with the validated dummy model run as a reference.

The accelerations and belt forces of an additional run with the energy absorbing back strap are presented in Figure 12. The maximum head excursion for this run was found to be 47 cm, compared to the 29 cm for the reference run.

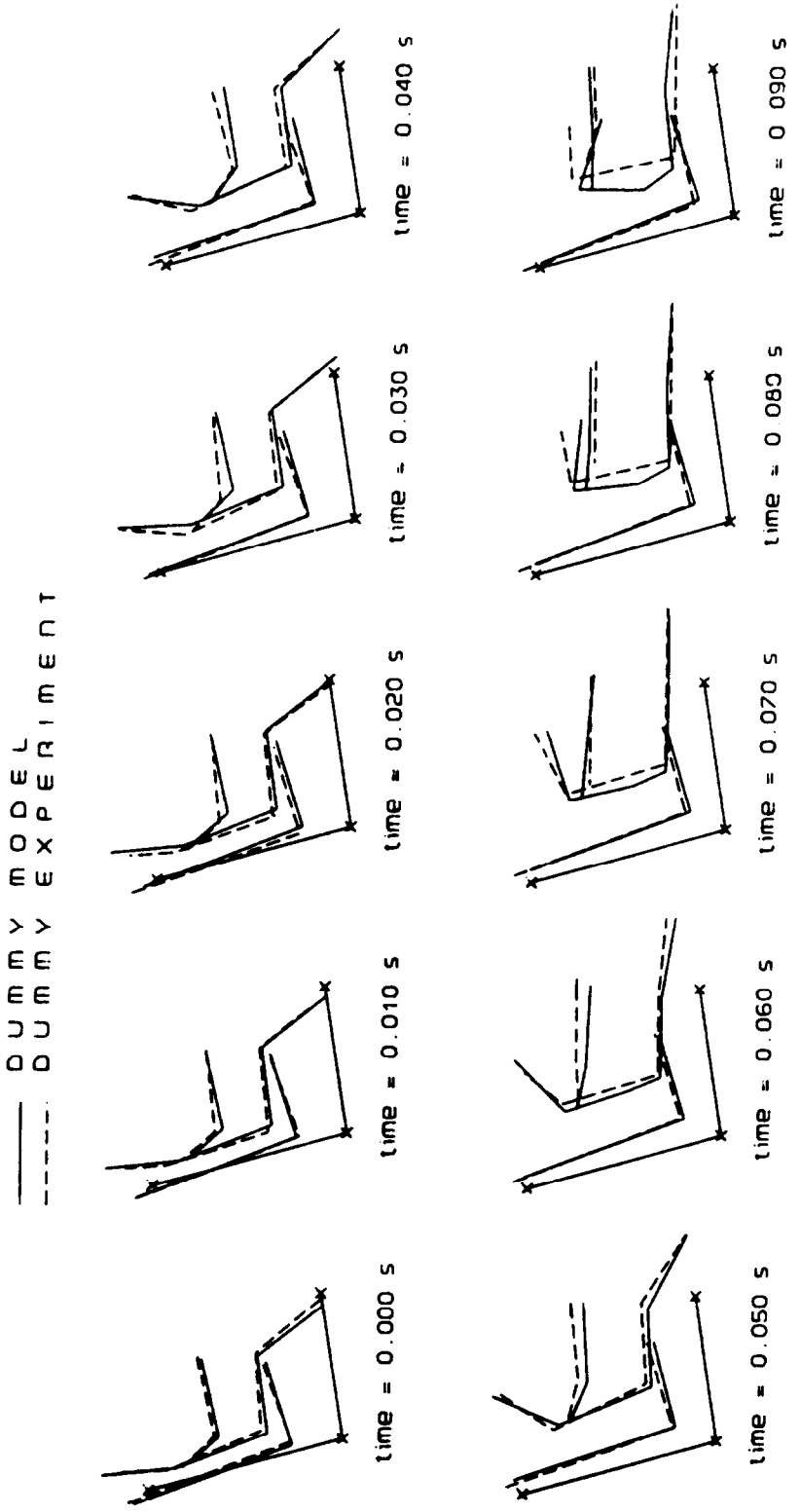

Fig. 8 - Comparison of kinematics of the dummy experiment with dummy model predictions

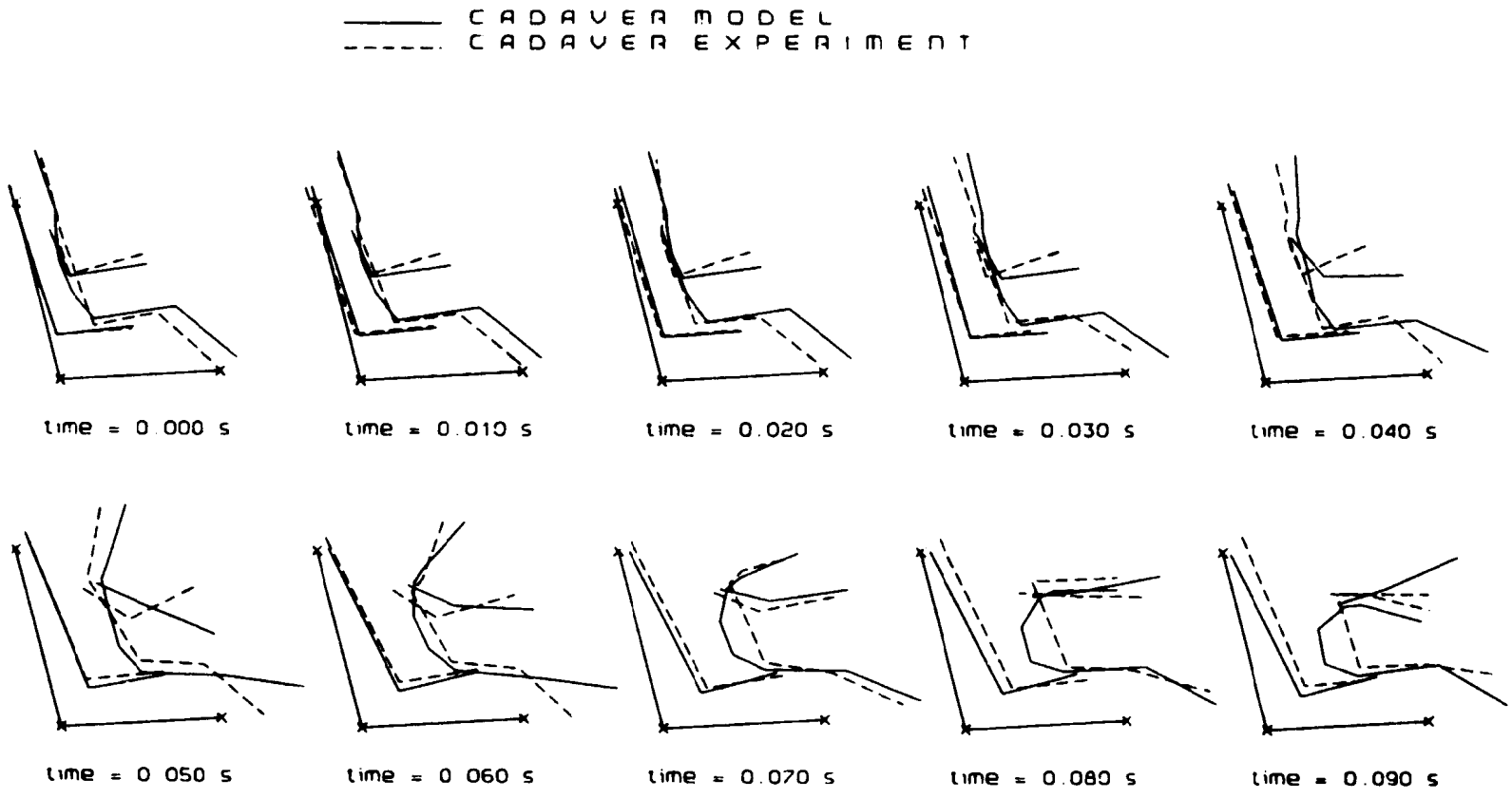

Fig. 9 - Comparison of kinematics of the cadaver experiment with cadaver model predictions

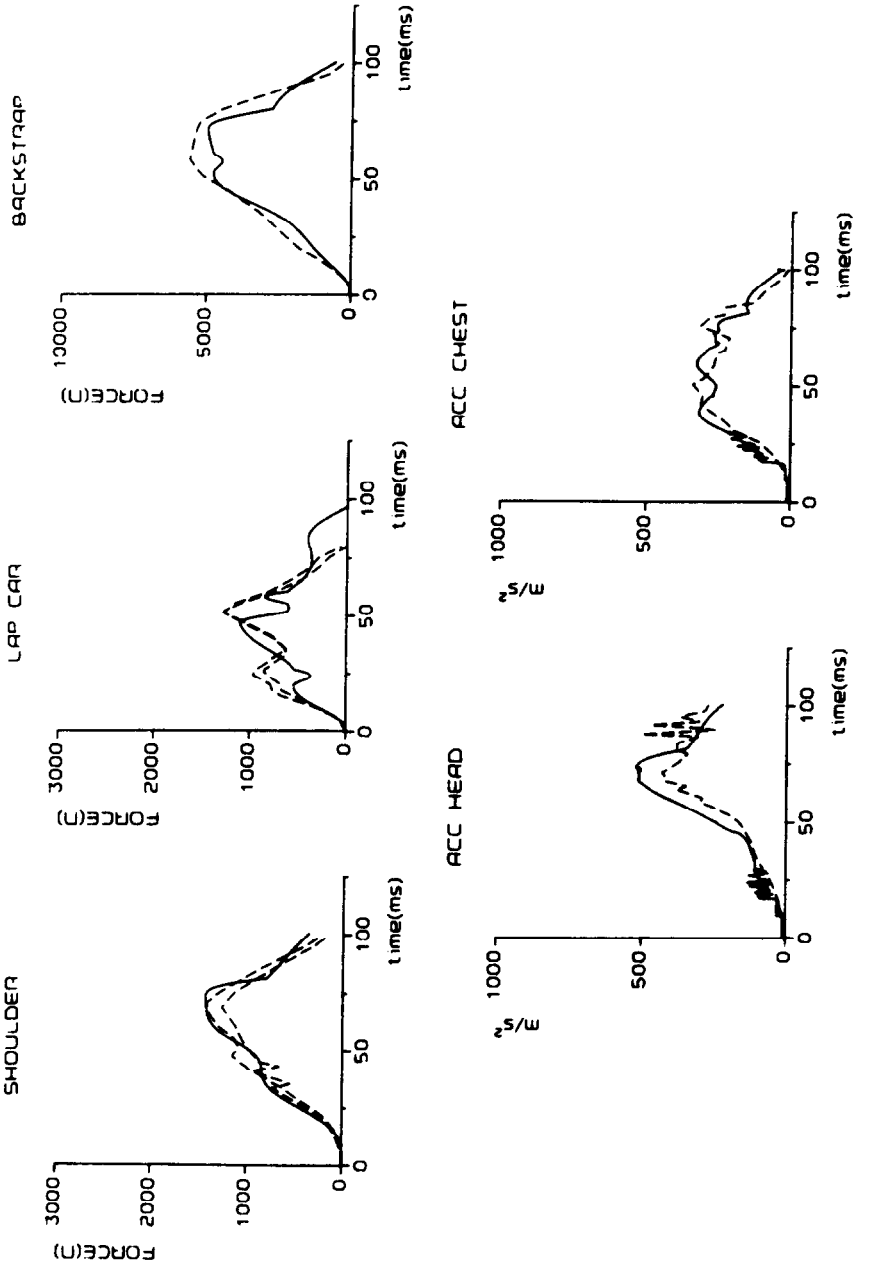

Fig. 10 - Comparison of belt forces and resultant accelerations of the dummy experiment with dummy model predictions

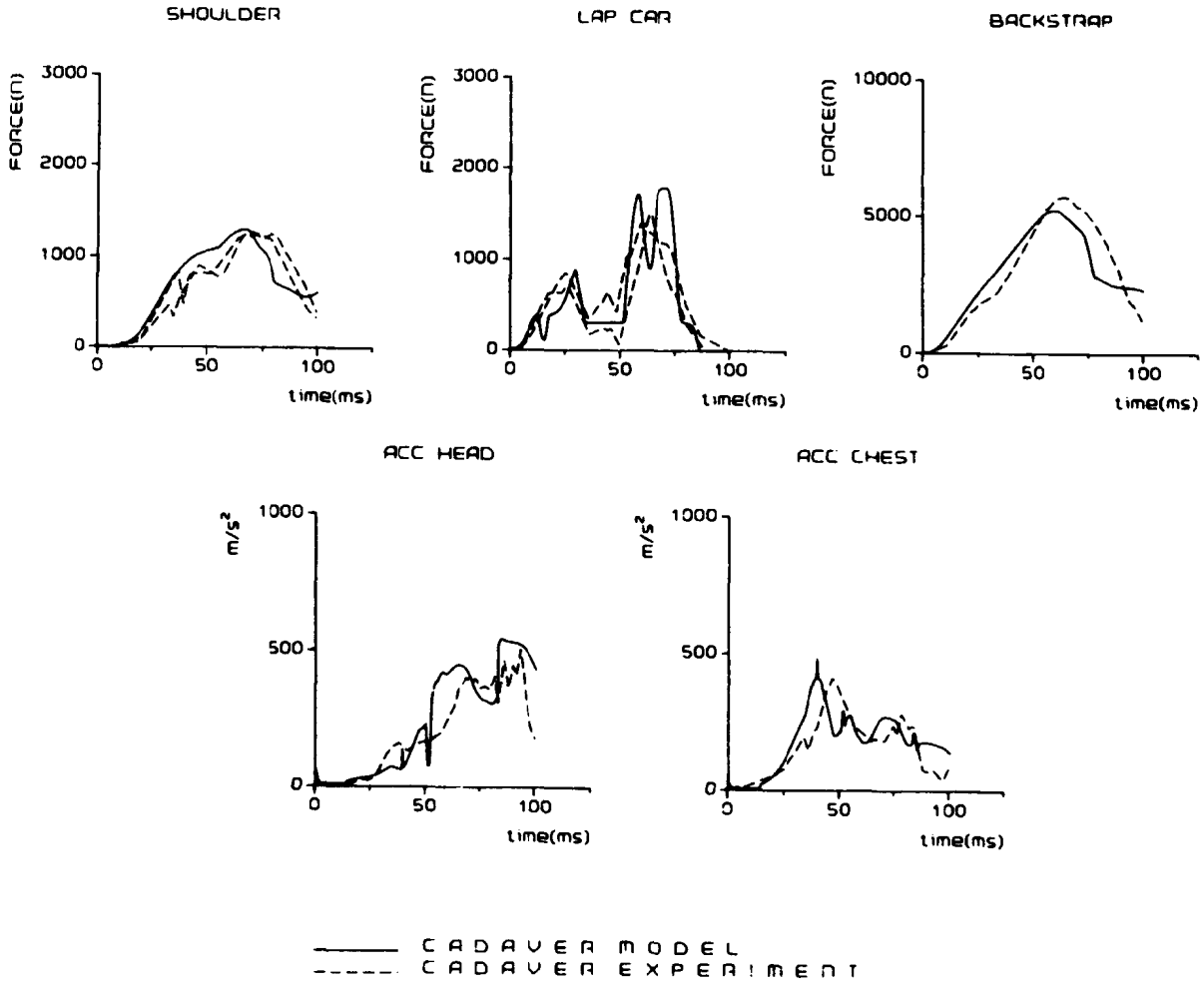

Fig. 11 - Comparison of belt forces and resultant accelerations of the cadaver experiment with cadaver model predictions

Table 9 - Head Excursion, Resultant Linear Accelerations and HIC of Experiments and Models.*

	Max Head Excursion		Max Head Acceleration		Max Chest Acceleration		
	cm	msec**	m/sec^2	msec	m/sec^2	msec	HIC
Cadaver experiment	37	82	400(507)***	75(94)	412	48	347
Cadaver model	36	85	449(548)	65(85)	410	40	614
Dummy experiment	29	85	433	71	340	53	349
Dummy model	30	80	521	73	323	60	457

*The maximum accelerations are calculated at the center of gravity. The chest acceleration is considered for intervals whose duration is 3 msec or more. The head excursion is measured relative to the forward most point on the vehicle seat back (FMVSS 213, March 1974).
**Time at peak value.
***Second peak, due to head-armrest contact.

Table 10 - Influence of Several Parameters on Occupant's Response:Based on the Validated Dummy Model

Parameter variation	Change in Maximum Head Excursion %	Head Acceleration %	Chest* Acceleration %	Shoulder Belt Load %	Car Lap Belt Load %	Backstrap Load %
1. Displacement of head c.g. lowered 2cm	0	- 4	+ 1	+ 2	- 1	+ 2
2. Displacement of head c.g. raised 2cm	0	+13	0	0	- 1	- 1
3. Friction coefficient in shoulder harness: 0 (free slipping)	+26	-16	- 1	-13	- 2	0
4. Friction coefficient in shoulder harness: 0.6 (increased by 33%)	- 8	0	0	+ 6	- 1	+ 4
5. Stiffness shoulder harness increased by 100%	-20	- 5	- 2	+ 9	+29	- 6
6. Stiffness shoulder harness decreased by 50%	+29	-11	- 4	-10	-37	+ 3

*The chest acceleration is considered for intervals whose duration is 3msec or more.

DISCUSSION

EXPERIMENTS - Because only one test on one cadaver was conducted, definite conclusions can not be made from the autopsy report. Nevertheless the loads on the chest were high enough to cause a possible flailed chest. Although no neck or groin injuries were observed, the question of neck and groin injuries by the use of 5-point harness is not resolved.

The tests in this study were conducted before the present United States proposed child restraint standard FMVSS 213, May 1978 was released. The only major difference between the testing procedures in the 1974 and 1978 proposed standards is the use of the standard bench seat. The fact that the standard bench seat-back is deformable, makes any comparison of the results between the two proposed standards questionable.

MODEL VALIDATION - Detailed measurements were done on the three-year old child dummy and the child cadaver. Together with additional assumptions this results in two datasets that can be used in crash victim models (2-dimensional).

The kinematics of the dummy model compared to the dummy experiment showed almost identical paths with respect to time (Fig. 8). The maximum head excursions and the corresponding times showed only small differences (Table 9). Shoulder harness and backstrap loads, as well as the resultant linear chest accelerations, all showed similar paths (Fig. 10). In the resultant linear head accelerations and the car lap belt loads, deviations were observed. The maximum linear head acceleration (at 71 msec) was 20% higher for the model simulation.

The kinematics of the cadaver model and the cadaver experiment, also showed similar paths with respect to time; but not as close as for the dummy comparison (Fig. 9). The maximum head excursions and the corresponding times, showed again, only small differences (Table 9). The shoulder harness belt loads, backstrap and car lap belt loads, as well as the chest accelerations showed similar time paths (Fig. 11). As in the dummy comparison there were differences observed in the head acceleration; a deviation of 12% for the first peak and 8% for the second (head contact with the child seat arm rest).

HIC value calculations for dummy model and cadaver model results were carried out. Both calculations showed large differences compared to the HIC values calculated for the experiments (Table 9). The HIC value was 31% higher for the dummy model and 77% higher for the cadaver model, while differences in peak head accelerations were 20% for the dummy model and 12% for the cadaver model. Similar differences between peak head accelerations and HIC values

were shown by Chou and Prasad (17). For the moment it is not clear what HIC correspondence is required for a satisfactory validation. This problem is under study by the Analytical Human Simulation Task Force of the SAE Human Biomechanics and Simulation Subcommittee. Until this work is completed, little relevance can be placed on this parameter as an indicator of validation.

Within the scope of this paper, the comparisons between the kinematics and dynamics of the models to the experiments were judged to be adequate. Based on this, the models were considered to be validated and can be used to study differences between the dummy and cadaver responses.

SENSITIVITY STUDY - The sensitivity study showed that changes in some of the estimated values, used in the models, could cause significant change in the dummy model response (Table 10). The head centre of gravity location, not well defined for the cadaver, was raised and lowered by two centimeters (Tables 10, 1 and 2). No significant changes in belt loads, chest acceleration and head excursions were found. The peak head acceleration, however, appeared to be sensitive to displacements of the head c.g. This could account for part of the deviations observed in the head acceleration of the cadaver model. The friction coefficient between the shoulder and the harness appeared to be an important parameter. A small change in the friction coefficient, which may occur in routine testing with an unclothed dummy, was found to be unimportant (Table 10, no. 3). However, the absence of friction (free slippage), as for example a dummy with multiple layers of cloths, has a large influence on the systems response (Table 10, no. 4). This factor should be considered when establishing test conditions for standards or restraint system evaluations.

Changes in the estimated values of the harness stiffness correction factor, to account for structural deformations, can have a large influence on the kinematics and dynamics of a simulation (Table 10, no. 5, 6). Differences were observed in the car lap belt load-time characteristics between the dummy model and dummy experiment. These differences were, at least in part, due to not being able to define accurately the harness stiffness correction factors. Variation in the head accelerations of the dummy and cadaver models could also be attributed to these factors.

ENERGY ABSORBING BACKSTRAP - The results of changing the backstrap in the dummy model from the standard belt to an energy absorbing belt showed an appreciable reduction of the peak and/or average forces and accelerations on the dummy model (Fig. 12). The head excursion increased, but by a controled amount designed into the backstrap. The increase in the head excursion was chosen to be 18 cm; this was still within the limit set by proposed FMVSS 213,

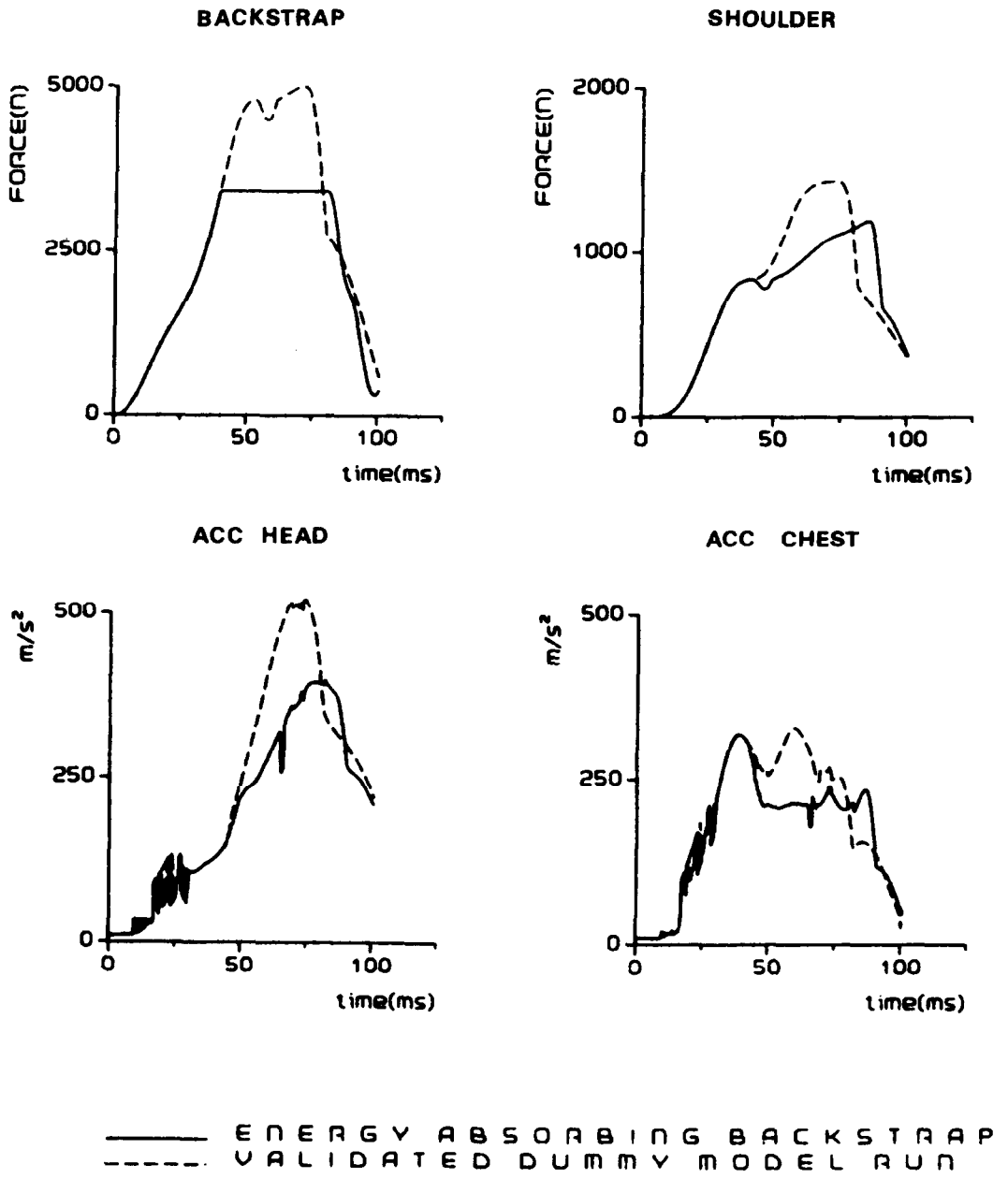

Fig. 12 - Influence of energy absorbing backstrap on belt forces and resultant accelerations

March 1974.

It was found in the autopsy that the chest of the cadaver was almost flailed. It could be inferred from this exercise that with lower shoulder belt loads (chest loads) and lower chest accelerations the probability of chest injury would be reduced. Lower head acceleration was also observed, which would indicate a lower probability of brain and neck injuries.

HUMAN SURROGATES - The most significant difference between dummy and cadaver response in this test configuration was in the motion of the head and upper torso.

The cadaver exhibited larger forward head excursions (37 cm as compared to 29 cm for the dummy) The motion of the head and upper torso of the cadaver was also greater in the downward direction at maximum forward excursion, causing the face of the cadaver to strike the armrest of the child seat. The dummy did not strike the armrest due to its more limited motion. By the cadaver model however, the kinematics of the cadaver test are predicted very realistic (Fig. 13).

Cadavers can be considered as surrogates for the living human being (18). Shortcomings of the cadaver in this respect are:

(1) Decrease of mechanical strength with age.
(2) Lack of muscle tone.
(3) Differences in body properties.

For this study with the child cadaver shortcomings (1) and (2) are not of a big relevance and shortcoming (3) is minimized by the applied testing techniques, like pressurization. So it is believed that a child cadaver is a reasonable surrogate for a living child. Since both the dummy experiment as well as the mathematical model of the cadaver can be considered as a surrogate for the living child, it is concluded that the cadaver model gives a more realistic simulation for the kinematics than the dummy experiment.

CONCLUSIONS

1. For this cadaver, tested in this manner, no neck or groin injury was detected, but a possible flailed chest was observed.
2. A 7-mass child dummy model and a 9-mass child cadaver model could be developed and validated for a specified test set up.
3. The predictions of both models agree quite well with the experimental test results.
4. The mathematical model gives a better simulation for the kinematics of a specific cadaver than a dummy experiment.
5. For a more realistic mathematical simulation, some

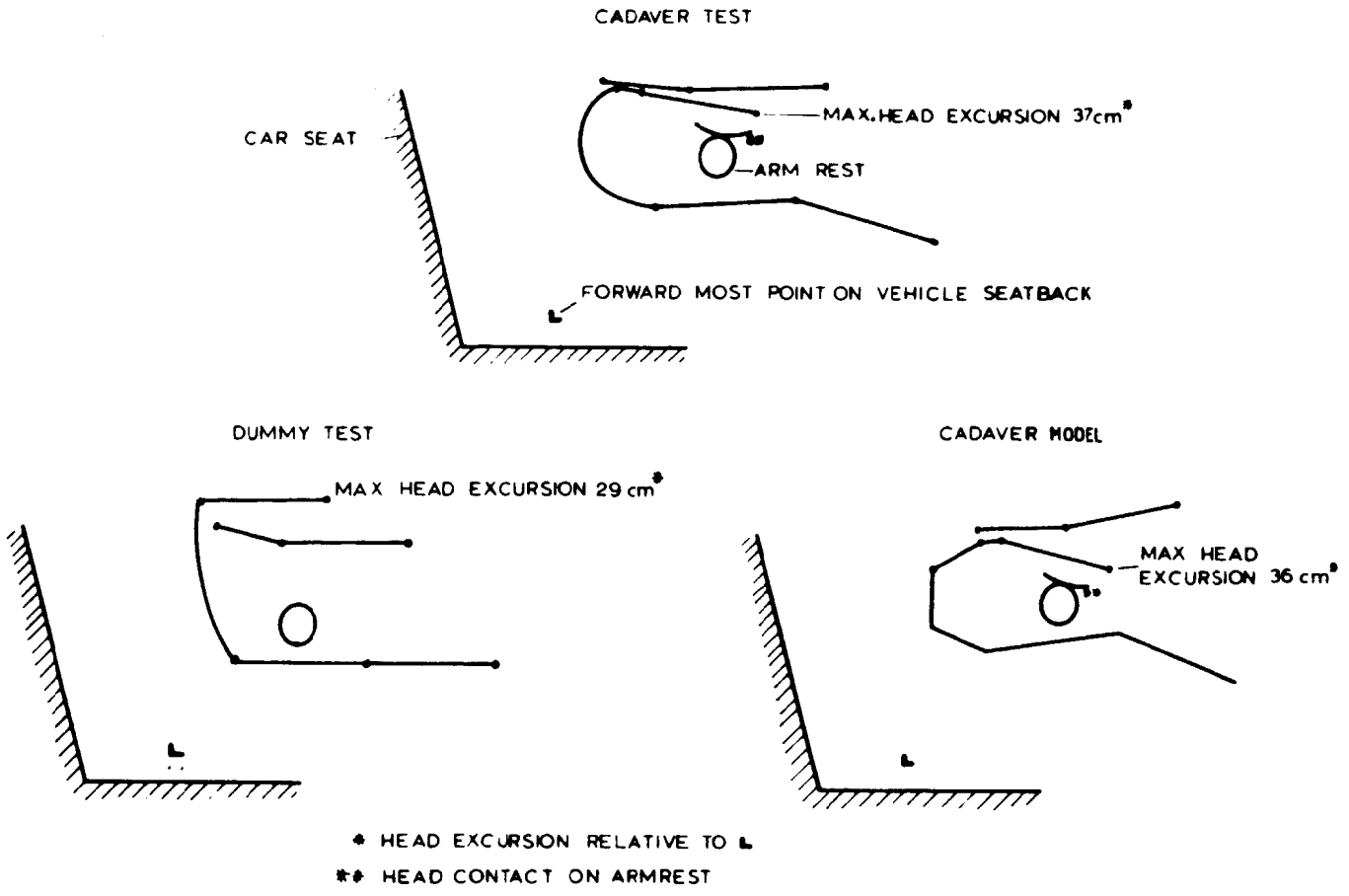

Fig. 13 - Comparison of the kinematics of the cadaver test with the kinematics of respective dummy test and cadaver model at time of maximum head excursion

refinements in the model have to be introduced and more detailed measurements for the input data are required.

6. The mathematical model can be employed to optimize child restraint systems.

ACKNOWLEDGEMENTS

MADYMO has been developed at the Research Institute for Road Vehicles TNO, Delft, Holland in collaboration with the Netherlands Institute for Road Safety Research SWOV. This is a six-year program sponsored by the Dutch government. The authors would like to acknowledge Mr. L. Wittebrood and Mr. H. Blok for their efforts running the MADYMO computer program and development of the graphical output programs and Mrs. R. Fa-Si-Oen for typing the manuscript. The assistance of Mr. Guy Nusholtz and Mr. Jeff Axelrod in the preparation and conduct of the experimental work and of Dr. Marvin Kirsh, Dr. Richard Burney and Dr. Donald Huelke in the injury evaluation are gratefully acknowledged.

REFERENCES

1. R.G. Snyder, D.R. Foust and B.M. Bowman, "Study of Impact Tolerance Through Freefall Investigations." Final Report prepared for the Insurance Institute for Highway Safety. UM-HSRI-77-8, Highway Safety Research Institute, the University of Michigan, Ann Arbor, Michigan, 1977.

2. D. Kallieris, J. Barz, G. Schmidt, and R. Mattern, "Comparison Between Child Cadavers and Child Dummy by Using Child Restraint Systems in Simulated Collisions." 22th Stapp Car Crash Conference, 1976. Society of Automotive Engineers, Inc., Warrendale, Pa.

3. B. Friedel, "Research Association for Biomechanics at the Federal Highway Research Institute." IRCOBI Conference, 1977.

4. N.M. Alem, B.M. Bowman, J.W. Melvin and J.B. Benson, "Whole-Body Human Surrogate Response to Three-Point Harness Restraint." Proceedings of the 22th Stapp Car Crash Conference, SAE Paper No. 780895, 1978. Society of Automotive Engineers Inc., Warrendale, Pa.

5. R.L. Stalnaker, J.W. Melvin, G.S. Nusholtz, N.M. Alem and J.B. Benson, "Head Impact Response." Proceedings of the 21th Stapp Car Crash Conference, SAE Paper No. 770921, Society of Automotive Engineers, Inc., Warrendale, Pa.

6. D.H. Robbins, J.W. Melvin, and R.L. Stalnaker, "The Prediction of Thoracic Injuries." Proceedings of the 20th Stapp Car Crash Conference, SAE Paper No. 760822, Society of Automotive Engineers, Inc., Warrendale, Pa.

7. R.L. Stalnaker, et.al., "Performance Evaluation of Child Dummies and Baboons in Child Restraint Systems in a

Systematized Crash Environment." Proceedings of the 19th Stapp Car Crash Conference, 1975. Society of Automobile Engineers, Inc., Warrendale, Pa.

8. D.H. Robbins, "Simulation of Human Body Response to Crash Loads." In Shock and Vibration Computer Programs. Monograph No. SVM-10, Shock and Vibration Computer Center, U.S. Dept. of Defense, pp. 365-380, 1975.

9. J.T. Fleck, F.E. Butler, S.L. Vogel, "Three-Dimensional Computer Simulation of Motor Vehicle Crash Victims." Report Cal.No. VJ-2978. V-2, Calspan Corp., Buffalo New York, 1974.

10. A.C. Bacchetti, J. Maltha, "Madymo a General Purpose Mathematical Dynamical Model for Crash Victim Simulation." Research Institute for Road Vehicles, The Netherlands, reportnr. 753012-C, 1978.

11. J.S.H.W. Wismans, J. Maltha and R.L. Stalnaker, "Construction, Validation and Sensitivity Analyses of a Child-Child Restraint Model." Research Institute for Road Vehicles TNO, Delft, The Netherlands, reportnr. 700120002-B, 1979 (in Progress).

12. K.N. Naab, "Measurement of Detailed Inertial Properties and Dimensions of a 50th Percentile Anthropometric Dummy." 10th Stapp Car Crash Conference, 1966. Society of Automotive Engineers, Inc., Warrendale, Pa.

13. J.A. Bartz, "Validation of a Three-Dimensional Mathematical Model of the Crash Victim." In: "Human Impact Response" ed. W.F. King, H.J. Mertz, p.346-379, 1973.

14. H.M. Reynolds, J.W. Young, J.T. Mc Conville and R.G. Snyder, "Development and Evaluation of Masterbody forms for Three-Year old and Six-Year old Child Dummies." Final Report DOT HS-801 811, 1976.

15. D.H. Robbins, R.O. Bennett and J.M. Becker, "Validation of Human Body Modeling for Dynamic Simulation." International Automotive Engineering Congress and Exposition, Detroit, SAE nr.: 770058, 1977.

16. S.H. Backaitis, "Sensitivity Study of Occupant Response in Simulated Crash Environment." SAE 740117, 1974.

17. C.C. Chou and P. Prasad, "Error Bounds on HIC for levels 2 and 4." Appendix B, SAE HBSS/AHSTF Meeting Notes, May 25, 1978.

18. "Human Injury Criteria as Related to Motor Vehicle Collisions." SAE Information Report J 885b (Draft), September 1978.